International Communications in Heat and Mass Transfer xxx (xxxx) xxx

Contents lists available at ScienceDirect

International Communications in Heat and Mass Transfer

journal homepage: www.elsevier.com/locate/ichmt

Falkner-Skan time-dependent bioconvrction flow of cross nanofluid with nonlinear thermal radiation, activation energy and melting process

Hassan Waqas [a], Shan Ali Khan [a], Sami Ullah Khan [b], M. Ijaz Khan [c], Seifedine Kadry [d], Yu-Ming Chu [e,f,*]

[a] Department of Mathematics, Government College University Faisalabad, Layyah Campus, Layyah 31200, Pakistan
[b] Department of Mathematics, COMSATS University Islamabad, Sahiwal 57000, Pakistan
[c] Department of Mathematics and Statistics, Riphah International University, I-14, Islamabad 44000, Pakistan
[d] Department of Mathematics and Computer Science, Beirut Arab University, Beirut, Lebanon
[e] Department of Mathematics, Huzhou University, Huzhou 313000, PR China
[f] Hunan Provincial Key Laboratory of Mathematical Modeling and Analysis in Engineering, Changsha University of Science & Technology, Changsha 410114, PR China

ARTICLE INFO

Keywords:
Falkner-skan flow
Cross nanofluid
Nonlinear thermal radiation
Activation energy
Numerical scheme

ABSTRACT

Owing to the dyanamic applications of nanoparticles in various bio-medical and engineering apllications like cancertheropy, microelectronics, energy storage devices, cooling and heating processes, the researchers have intended their focus toward this topic. On this end, the motivating objective of current communication is to investigate the Falkner-Skan bioconvection flow of cross nanofluid conformist with melting phenomenon over a moving wedge. The impact of activation energy and nonlinear thermal radiation are also addresed. The famous Buongiorno model is utilized for thermophoretic and Brownian asesment analysis. The governing equations for time dependent Falkner-skin flow of cross fluid mathematical models are simplified into a dimensionless coupled system of ordinary differential expressions by applying adequate similarity transformation. The developed subsequent differential system is solved numerically through engaged shooting solver in computational software MATLAB. The graphical analysis against flow parameters has been performed against velocity, nanofluid temperature, conctration profile and gytoractic microorganisms.

1. Introduction

The dilute suspension of metallic nano-sized particles with base materials are reffered to the nano-materials and has become attractive research area for dynamic scientists. The composites made of nanoparticles have changed the physical characteristics of the fluid when compared to ordinary liquids. In all these aspects, the thermal conductivity and other flow feature are an extremely physical consequences. The renewable and novel applications of nanofluid include heat transfer devices, material, medical sciences, electronic, catalysis, optics, smart computers, development, renewable and many other applications. From a convenient application point of analysis, nanofluid is used in powered engines, pharmaceutical processes, micro electrons and hybrid fuel cells. It is currently important for the industry to use electronic devices and nanoboards. In addition, nanofluid is a new type of energy transfer fluid that is the suspension of base fluids and nanoparticles. Natural heat transfer fluids cannot be used for cooling requirements due to their lower thermal conductivity. By implanting nanoparticles into normal fluids, their thermal constitutionality can be significantly enhanced. The first publication introducing the concept of nanofluid is generally accepted by Choi [1]. Buongiorno [2] described the two important strategies known as thermophoresis force and Brownian motion, which are important factors in improving the ability of ordinary fluids to transport heat.Selimefendigilet et al. [3] studied the Hydrothermal of nonmaterial's transporting across a porous compound cavity using two temperature and heat transformation models under the magnetic field consequence. Rashid et al. [4] researched the stagnation point boundary layer movement of copper–water based nanoliquids that are relevant to the magnetic field. The joint impact of the magnetic field as well as the Marangoni convection vs the thin layer diesel fuel oil based carbon nanotubes nanoparticles by Gul et al. [5] has been scrutinized. Siddiqui et al. [6] explored the thermo magneto hydrodynamic impacts over nanoliquid flow in a porous circular annular area formed by two moving cylinders in the absence of a steady radial magnetic field although

* Corresponding author at: Department of Mathematics, Huzhou University, Huzhou 313000, PR China.
E-mail address: chuyuming@zjhu.edu.cn (Y.-M. Chu).

https://doi.org/10.1016/j.icheatmasstransfer.2020.105028

Please cite this article as: Hassan Waqas, *International Communications in Heat and Mass Transfer*, https://doi.org/10.1016/j.icheatmasstransfer.2020.105028

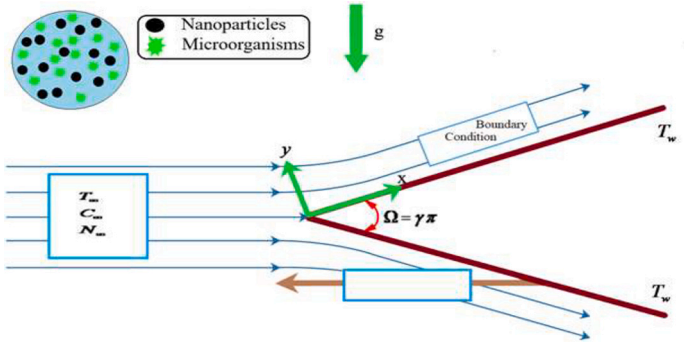

Fig. 1. Physical view of flow.

variable heat conductivity. Chen et al. [7] investigated Viscosity characteristics of graphite / engine oil nanofluid are experimentally tested. Ansariet et al. [8] described the flow process of Jeffrey nanofluid flow to the Riga board, incorporating viscous dissipation effects, erratic heat source/sink, Brownian motion and thermophoresis energy. Xian et al. [9] described Stable hybrid nanofluid have been developed by dispersing grapheme nanoplatelets (GnPs) and titanium dioxide (TiO2) in a mixture of purified water and ethylene glycol (DW / EG) using a two-step process. Alharbi et al. [10] show Wall slips impacts and wall temperature increases as thermal energy is passed to hybrid nanofluid. Khan et al. [11] examined the effectiveness of three-dimensional inclined MHD Carreau nanofluid flow past Human stagnation point with Darcy–Forchheimer and chemical reactive species. Nguyen et al. [12] used numerical methods to analyze the significant impacts of MHD flow and nanoparticles migration within permeable volume, including two temperature simulations. Rabbi et al. [13] developed the magneto-hydrodynamic thermal conduction in a square tub of Cu-H2O nonmaterial is examined for the various configurations of the thermostat-sink in which the Artificial Neural Network (ANN) method was used as an effective predictive method. Many researchers [14–16] addressed the significance of thermophoresis, as well as Brownian motion, with different physical features.

Activation energy is the smallest energy production required to conduct a chemical process.The term of activation energy is first time introduced bySvante Arrhenius in1889.He calculated the energy to be eradicated from chemical reactions named activation.The minimum energy required to start some chemical reaction is often recognized as activation energy.There are Numerous applications in mass transformation phenomena followed by chemical reactions through activation energy involve geothermal reservoirs, mechanical engineering, food manufacturing, oil and water emulsion technology, respectively.In general the Activation energy is represented by E_a. Bestman [17] investigated the activation-energy impact in fluid. Shah et al. [18] explored the Radiative Magneto hydrodynamic Casson nanoliquid flow including activation energy and chemical processes by Entropy generation through past nonlinear stretched surfaces. Muhammad et al. [19] determined fully established Darcy-Forchheimer mixed convective flux via curved surface including activation energy. A 3-dimensional mathematical study of Eyring–Powell Nanoliquid Nonlinear thermal energy with improved heat and mass fluxes is analyzed Muhammadet al. [20]. Khan et al. [21] examined the activation energy characteristics of magnetic material Cross nanofluid applied to cylindrical surface. Bhatti et al. [22] researched deals by the swimming of motile microorganisms in a nanoliquid over a stretching surface.

The macroscopic acceleration of the fluid due to the gradient of density created by the continuous swimming of motile microorganisms is known as bioconvection. Gyrotactic microorganisms are inserted in nanofluid to facilitate fluid mixing as these organisms are responsible for the bioconvection cycle. Such organisms are smaller than water and usually move in the opposite direction of the gravity. Bioconvection is a natural process created by the spontaneous movement of microorganisms in individual cells or in a cell-form community. Platt (1961) first invented the word “bioconvection” in his research, stating the patterns of flow found in the culture of free-swimming species [23]. In the Tetrahymena history, he found movable polygonal structures that were identical to the Benard cells. However, extensive works can be found in refs [24–28]. Shamshuddin et al. [29] analyzed analytically three dimensional viscous time-dependent bioconvection in the spinning nanofluid flow through the rotating disc. Nadeem et al. [30] researched focus on the unsteady three dimensional forced bioconvection movement of a viscous liquid. Bioconvection Nanofluid (MHD) flow of nanofluid against a stretching sheet through velocity slip and viscous dissipation is observed by Ayodeji et al. [31]. Ahmed et al. [32] addressed a revised structure for the unsteady mixed micro-bioconvection flow in the horizontal channel including its upward plate extending. A mathematical structure for the bioconvection flow of Williamson nanoliquid via stretching cylinder with variable heat conductivity, activation energy as well as second-order slip are investigated by Abdelmalek et al. [33]. Bioconvection aspects in magnetized couple stress nanoliquidinvolving activation energy and second order slip was described by Khan et al. [34]. Waqas et al. [35] examined the bioconvection flow of nanoliquid is subject of concern in recent years as it includes a range of physical importance in biotechnology.Abdelmalek et al. [36] scrutinized the bioconvection process through the use of nonmaterial in fluid.Maxwell nanofluid including swimming microorganism and activation energy is describedby Waqas et al. [37].

Current work deals with the bioconvection Falkner-Skan flow of cross nanofluid induced by a wedge under the interesintg influence of melting heat transfer. The additional impact of thermal radiation and activation energy are also taken into account. The flow equations are altered into dimensionless forms which are numerically treated via shooting technique. The flow pattern is observed with help of different graphs and physical explanations.

2. Mathematical discruption

Consider a time-dependent Falkner-skin bioconvection flow of cross nanofluid induced by stretching wedge with angle $\Upsilon = \beta\pi$, free stream $U_w = \frac{bx^m}{1-ct}$ and streating velocity $U_e = \frac{ax^m}{1-ct}$ which a, b, c are constant as shown in Fig. 1. The aspects of activation energy and nonlinear thermal radiation are taken into account. When wedge is stretching, it satisfy $U_w(x,t) > 0$ while $U_w(x,t) < 0$ denotes the case of contracting. The ambient temperature is reflected by T_m, while ambient concentration and microorganism are denoted by C_m and N_m, respectively. Under the above attention boundary layer governing equations for Cross nanofluid with melting phenomenon are:

$$u_x + v_y = 0 \tag{1}$$

$$u_t + uu_x + vu_y = U_{e_t} + U_e U_{e_x} + \nu\left(\beta^* u_{yy} + (1-\beta^*)u_{yy}\left(\frac{1}{1+\Gamma^n\left(u_y\right)^n}\right)\right)$$
$$-n\nu(1-\beta^*)\Gamma^n\left(u_{yy}\right)^n\left(\frac{1}{1+\Gamma^n\left(u_y\right)^n}\right)+\frac{1}{\rho_f}\begin{bmatrix}(1-C_f)\rho_f\beta^* g(T-T_\infty)\\ -\left(\rho_p-\rho_f\right)g(C-C_\infty)\\ -(N-N_\infty)g\gamma^{**}\left(\rho_m-\rho_f\right)\end{bmatrix}, \tag{2}$$

$$T_t+uT_x+vT_y=\left(\alpha_m+\frac{16T_\infty^3\sigma^{**}}{3(\rho c)_f k^{**}}\right)T_{yy}+\tau\left\{D_B T_y C_y+\frac{D_T}{T_\infty}\left(T_y\right)^2\right\}+\frac{Q_0}{(\rho c)_f}(T-T_m), \tag{3}$$

$$C_t + uC_x + vC_y = D_B C_{yy} + \frac{D_T}{T_\infty}T_{yy} - Kr^2(C-C_\infty)\left(\frac{T}{T_\infty}\right)^m exp\left(\frac{-E_a}{\kappa T}\right), \tag{4}$$

$$N_t + uN_x + vN_y = D_m\left(N_{yy}\right) - \frac{bW_c}{(C_w - C_\infty)}\left(NC_{yy} + C_y N_y\right), \tag{5}$$

With boundary conditions

$$\left.\begin{aligned} u = sU_e,\ T = T_m,\ D_B C_y + \frac{D_T}{T_\infty}C_{yy},\ N = N_m \ \ at\, y = 0,\\ u\to U_e,\ \ T\to T_\infty,\ \ C\to C_\infty,\ \ N\to N_\infty \ \ as\, y\to\infty. \end{aligned}\right\} \tag{6}$$

The relation for melting heat conditions is

$$-k\left(T_y\right)\big|_{y=0} = \rho[\lambda + (T_m - T_0)c_s] \tag{7}$$

Let us introduce the variable to attain the dimensionless form of given equations

$$\left.\begin{aligned} \psi(x,y,t) = \sqrt{\frac{2\nu x U_e}{m+1}}f(\zeta), \zeta = y\sqrt{\frac{(m+1)U_e}{2\nu x}}\\ \theta(\zeta) = \frac{T-T_\infty}{T_m-T_\infty}, \phi(\zeta) = \frac{C-C_\infty}{C_m-C_\infty}, \chi(\zeta) = \frac{N-N_\infty}{N_m-N_\infty} \end{aligned}\right\}, \tag{8}$$

Replacing the above conversion parameters into the governing system of Falkner-Skin cross mathematical model, Eq. (1) is inevitably fulfilled while remaining equations are reduce to following system:

$$\beta^*\left((Wef'')^n+1\right)^2 f''' - \left(A(f'+0.5\zeta f''-1) - ff'' + \beta\left(f'^2-1\right)\right)(1+(Wef'')^n) + (1-(n-1)(Wef'')^n)(1-\beta^*)f''' + \alpha(\theta - Nr\phi - Nc\chi) = 0, \tag{9}$$

$$\left(\left(1+Rd(1+(\theta_w-1)\theta)^3\right)\theta'\right)+Prf\theta'-PrA\zeta\theta'+PrNb\theta'\phi'+PrNt\theta'2+PrQ\theta=0, \tag{10}$$

$$\phi'' + LePrf\phi' - LePrA\zeta\phi' + \left(\frac{Nt}{Nb}\right)\theta'' - PrLe\sigma(1+\varpi\theta)^m exp\left(\frac{-E_a}{1+\varpi\theta}\right)\phi = 0, \tag{11}$$

$$\chi'\prime + Lbf\chi' - Pe(\phi'\prime(\chi+\Omega)+\chi'\phi') = 0, \tag{12}$$

with

$$\left.\begin{aligned} f' = \lambda, \theta(\zeta) = 1, Nb\phi'(\zeta) + Nt\theta'(0) = 0, \chi(\zeta) = 1 \ \ at\ \zeta = 0,\\ f'\to 1, \theta(\zeta)\to 0, \phi\to 0, \chi(\zeta)\to 0 \ \ as\ \ \zeta\to\infty. \end{aligned}\right\} \tag{13}$$

futher dimensionless form of melting conditions:

$$M\theta + Prf = 0 \quad at \ \ \zeta = 0. \tag{14}$$

In the above equations, $We^2 = \frac{(m+1)\Gamma^2 U_c^3}{2\nu x}$is the local Weissenberg number, the Wedge angle parameter is denoted by$\beta = \frac{2m}{m+1}$, infinite shear rate viscosity is$\beta^* = \frac{\mu_\infty}{\mu_0}$,$\alpha = \frac{\beta^* g(1-C_\infty)(T_m-T_\infty)x}{(m+1)U_e^2}$stand for mixed convection parameter, buoyancy ratio parameter is expressed asNr = $\frac{\left(\rho_p-\rho_f\right)(C_m-C_\infty)}{\rho_f(1-C_\infty)(T_m-T_\infty)\beta^*}$, Nc = $\frac{\gamma^{**}\left(\rho_m-\rho_f\right)(N_m-N_\infty)}{\rho_f(1-C_\infty)(T_m-T_\infty)\beta^*}$ is the bioconvection Rayleigh number, $A = \frac{c}{(m+1)\alpha x^{m-1}}$the unsteideness parameter, the Prandtl number is simplified as $Pr = \frac{\mu c_p}{k}$,$Nt = \frac{\tau D_T(T_m-T_\infty)}{T_\infty\nu}$the thermophoresis parameter, radiation parameter is denoted by $Rd = \frac{16\sigma^{**}T_\infty^3}{3K_\infty k^{**}}$,$\theta_w = \frac{T_f}{T_\infty}$is temperature ratio parameter, $Nb = \frac{\tau D_B(C_m-C_\infty)}{\nu}$ the Brownian motion parameter, heat sink/source parameter is$Q = \frac{Q_0(1-ct)}{\rho c_p(m+1)\alpha x^{m-1}}$, Lewis number is represented by$Le = \frac{\alpha}{D_B}$, chemical reaction parameter is$\sigma = \frac{Kr^2}{\alpha x^{m-1}}$, tempreature difference parameter is read as $\varpi = \frac{T_m-T_\infty}{T_\infty}$, activation enegy is $E = \frac{E_a}{K_\infty T_\infty}$, bioconvection Lewis number is read as, $Pe = \frac{bW_c}{D_m}$ the Peclet number, microorganisms difference parameter is$\Omega = \frac{N_\infty}{N_m-N_\infty}$, velocity ratio parameter is $\lambda = \frac{b}{a}$and melting parameter is$M = \frac{c_p(T_m-T_\infty)}{\lambda+c_s(T_m-T_0)}$.

The physical quantities of interest are drag force, local Nusselt number and local microorganism density number, which are described as

$$\left.\begin{aligned} Cf_x = \frac{\tau_w|_{y=0}}{\rho U_e^2}, Nu_x = \frac{x}{(T_m-T_\infty)}\left(T_y\right)\big|_{y=0},\\ Sh_x = \frac{x}{(C_m-C_\infty)}\left(C_y\right)\big|_{y=0},\\ Sn_n = \frac{x}{(N_m-N_\infty)}\left(N_y\right)\big|_{y=0} \end{aligned}\right\}, \tag{15}$$

Dimensionless formof engineering physical quantities are:

$$\left.\begin{aligned} Re_x^{1/2}Cf_x = \sqrt{\frac{m+1}{2}}f''(0)\left[\frac{\beta^*+(1-\beta^*)}{1+(Wef''(0))^n}\right],\\ Re_x^{-1/2}Nu_x = -\sqrt{\frac{m+1}{2}}\theta'(0),\\ Re_x^{-1/2}Sh_x = -\sqrt{\frac{m+1}{2}}\phi'(0),\\ Re_x^{-1/2}Sh_n = -\sqrt{\frac{m+1}{2}}\chi'(0) \end{aligned}\right\} \tag{17}$$

3. Numerical approach

In this section, the transformed nonlinear differential dimensionless system (9–12) with boundries constraints (13–14) are numerically integrated by using shootinscheme knows as bvp4c solver with Lobatto-IIIa formula aid the commercial software Matlab. First the higher order system is tranformed into first order initial values problem by utilizing some new variables such as.

Let

$$\begin{aligned} f = r, f' = r_1, f'' = r_2, f''' = r_2',\\ \theta = r_3, \theta' = r_4, \theta'' = r_4',\\ \phi = r_5, \phi' = r_6, \phi'' = r_6',\\ \chi = r_7, \chi' = r_8, \chi'' = r_8'. \end{aligned} \tag{18}$$

$$r_2' = \frac{\left(A(r_1+0.5\zeta r_2-1)+rr_2-\beta\left(r_1^2-1\right)\right)(1+(Wer_2)^n)-\alpha(r_3-Nrr_5-Ncr_7)}{\left(\beta^*\left((Wer_2)^n+1\right)^2+(1-(n-1)(Wer_2)^n)(1-\beta^*)\right)}, \tag{19}$$

$$\begin{aligned} r_1 = \lambda \qquad & at\ \zeta = 0,\\ r_1\to 1 \qquad & as\zeta\to\infty. \end{aligned} \tag{20}$$

$$r_4' = \frac{-Prrr_4 + PrA\zeta r_4 - PrNbr_4r_6 - PrNtr_4^2 - PrQr_4}{\left(1+Rd(1+(\theta_w-1)r_3)^3\right)}, \tag{21}$$

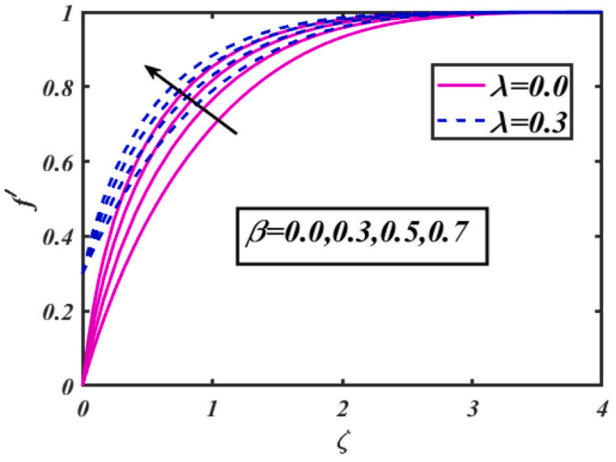

Fig. 2. Aspects of f' viaβ.

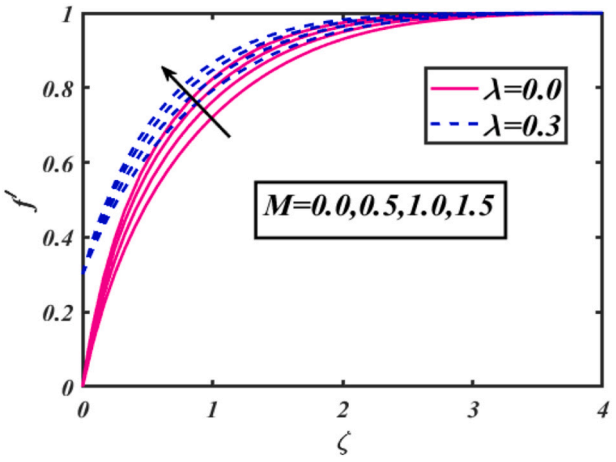

Fig. 3. Aspects of f' via$M$.

$$\begin{matrix} r_3(\zeta) = 1 & at\ \zeta = 0, \\ r_3(\zeta) \to 0 & as\ \zeta \to \infty. \end{matrix} \tag{22}$$

$$\phi'' = -LePrrr_6 + LePrA\zeta r_6 - LePr\left(\frac{Nt}{Nb}\right)r_4' + PrLe\sigma(1+\varpi r_3)^m exp\left(\frac{-E_a}{1+\varpi r_3}\right)r_5 \tag{23}$$

$$\begin{matrix} Nbr_6(\zeta) + Ntr_4(0) = 0, & at \quad \zeta = 0, \\ r_5 \to 0 & as \quad \zeta \to \infty. \end{matrix} \tag{24}$$

$$r_8' = -Lbrr_8 + Pe\left(r_6'(r_7 + \Omega) + r_8 r_6\right), \tag{25}$$

$$\begin{matrix} r_7(\zeta) = 1 & at \quad \zeta = 0, \\ r_7(\zeta) \to 0 & as \quad \zeta \to \infty. \end{matrix} \tag{26}$$

$$Mr_3 + Prr = 0 \qquad at \quad \zeta = 0. \tag{27}$$

4. Discusson

The physical exploration for characteristics of various parameters like local Weissenberg number *We*, melting parameter *M*, mixed convection parameter α, bioconvection Rayleigh number *Nc*, buoyancy ratio parameter *Nr*, wedge angle parameter β, Prandtl number *Pr*, Brownian motion parameter *Nb*, thermophoresis parameter *Nt*, Lewis number *Le*, temperature ratio parameter θ_w, bioconvection Lewis number *Lb* and Peclet number *Pe* is disclosed in this section. Since this work is theoretical therefore, all the parameters have assigned some fixed artibrary values [38–40]. The performances of wedge angle parameter β against velocity field f' of Falkner-Skan cross nanofluid for static and moving wedge are depicted in Fig. 2. This figure manifest that the variations of velocity profilef' increases by improving the magnitudes of wedge angle parameter $\beta$for both situations static and moving wedge. Fig. 3 is drawn

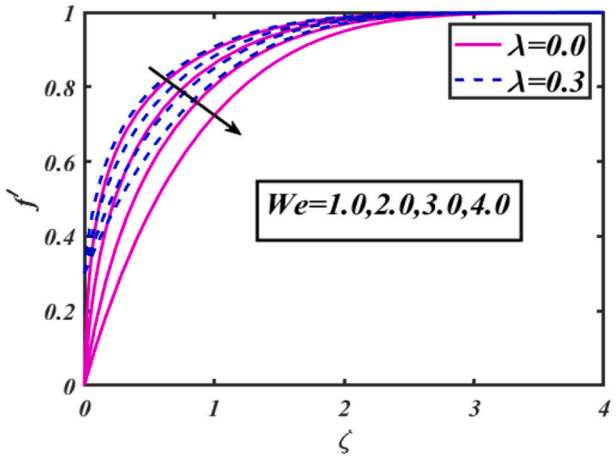

Fig. 4. Aspects of f' viaWe.

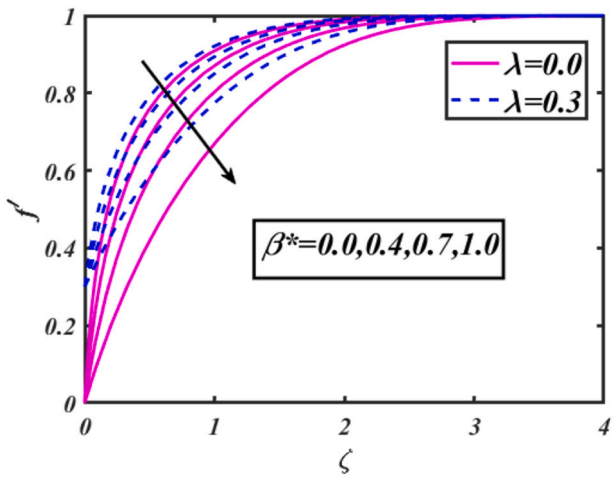

Fig. 5. Aspects of f' viaβ^*.

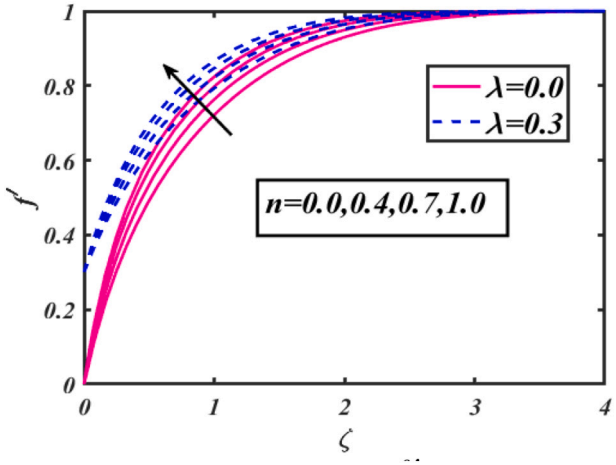

Fig. 6. Aspects of f' via$n$.

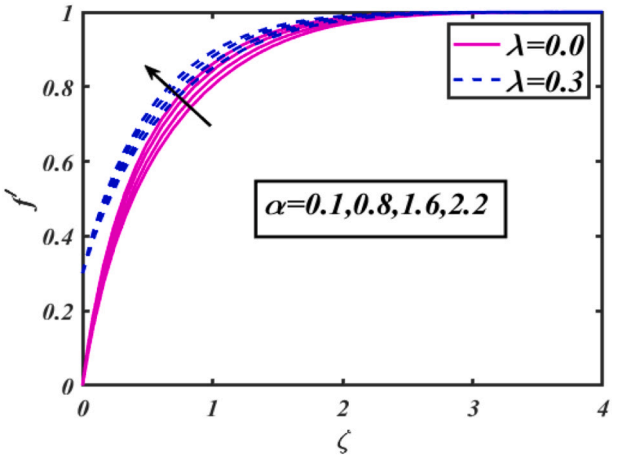

Fig. 7. Aspects of f' via α.

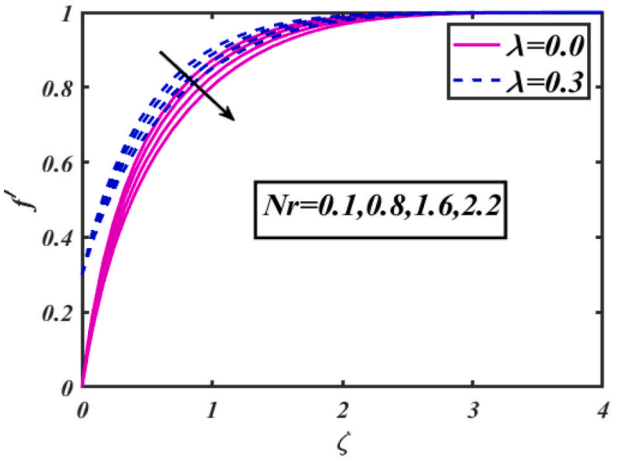

Fig. 8. Aspects of f' via Nr.

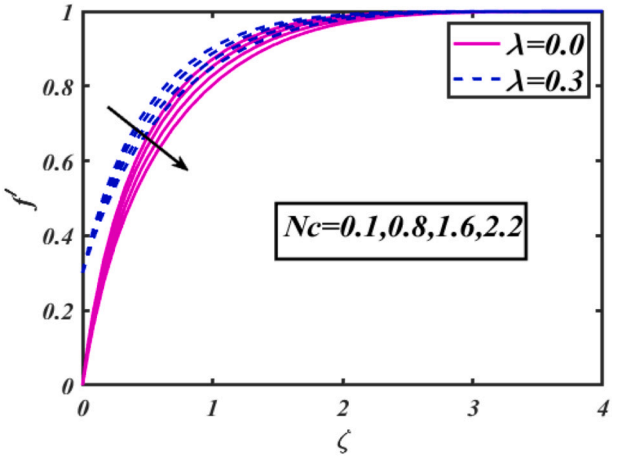

Fig. 9. Aspects of f' via Nc.

to investigate the feature of velocity field f' against melting parameter M for both cases. It is perceived that velocity of Falkner-Skan cross fluid f' increases for larger melting parameter M. The characteristics of velocity field f' versus larger Weissenberg number We is depicted in Fig. 4. Here, velocity of fluid f' dwindles with higher Weissenberg number We. The outcomes of velocity profile f' with larger infinite shear rate viscosity

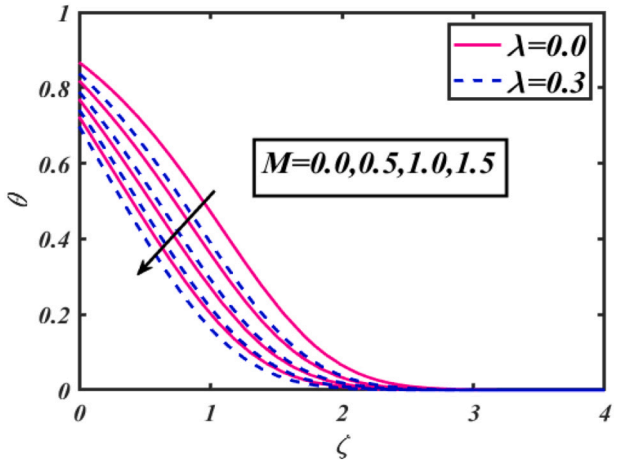

Fig. 10. Aspects of θ via M.

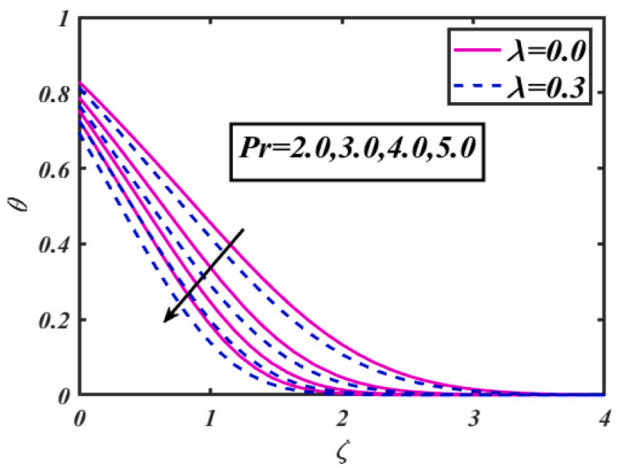

Fig. 11. Aspects of θ via Pr.

parameter β^* are presented in Fig. 5. Here flow of fluid f' declines for infinite shear rate viscosity parameter β^*. Fig. 6 is captured to examine the effect of power law-index n on velocity field f' for static and moving wedge. It is witnessed that velocity of fluid f' enhanced for larger power law-index n. Fig. 7 represents the impacts of mixed convection parameter α on flow of Falkner-Skan cross nanofluid f' over a Wedge, for both

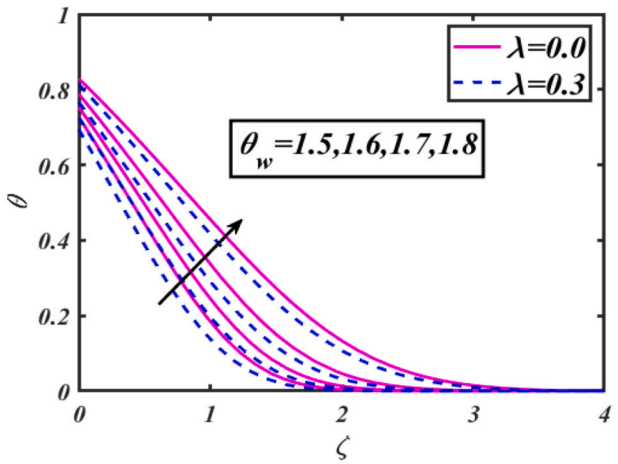

Fig. 12. Aspects of θ via θ_w.

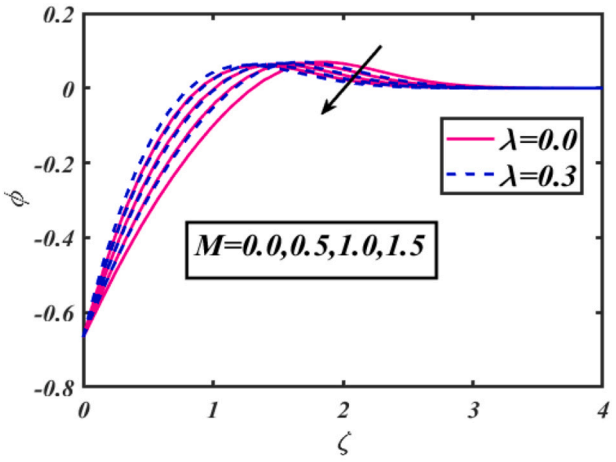

Fig. 13. Aspects of ϕvia$M$.

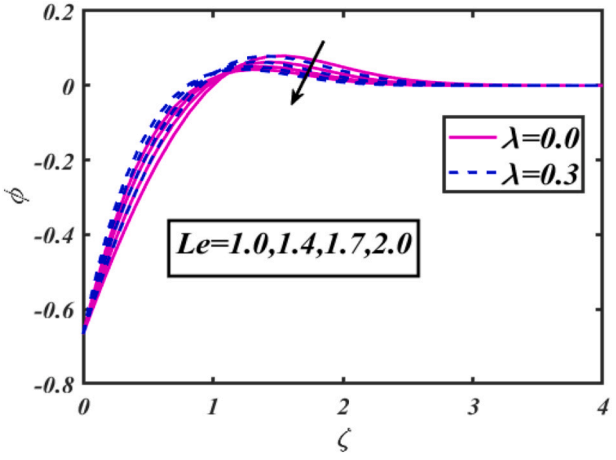

Fig. 14. Aspects of ϕviaLe.

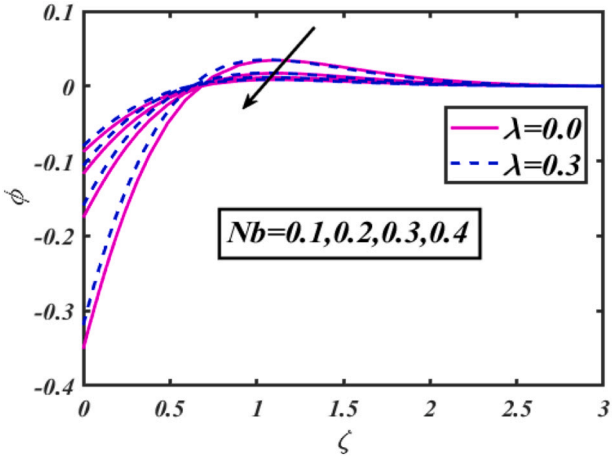

Fig. 15. Aspects of ϕviaNb.

cases $\lambda = 0.0$ and$\lambda = 0.3$. It is clear that by increasing the magnitudes of mixed convection parameterα the velocity fieldf' raises. Fig. 8 is drawn to check out the behavior of buoyancy ratio parameterNr on velocity of cross nanofluid f'through a wedge. It is found that velocity fieldf' depreciates by improving the estimations of buoyancy ratio parameterNr accordingly to the both cases static and moving wedge. Fig. 9 is sketched

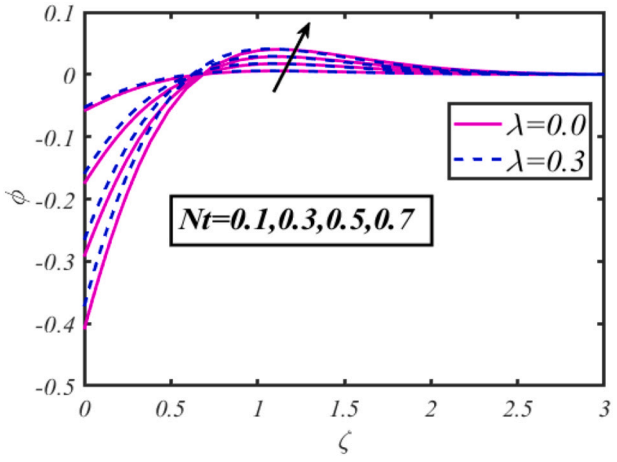

Fig. 16. Aspects of ϕviaNt.

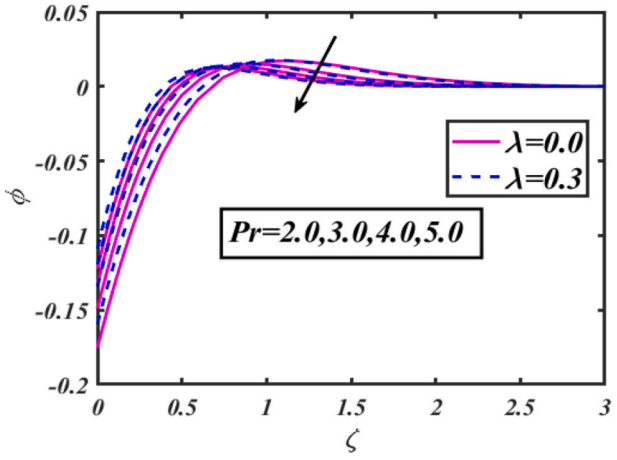

Fig. 17. Aspects of ϕviaPr.

to illustrate the inspiration of bioconvection Rayleigh numberNc on flow of Falkner-Skan cross modelf' over static $\lambda = 0.0$and move $\lambda = 0.3$wedge situations. From this picture, it is noticeable velocity of fluid f'diminishes for larger magnitudes of bioconvection Rayleigh numberNc. Consequence of melting parameter $M$for temperatureθ is portrayed through Fig. 10. It is interesting to notice that temperature field $\theta$of Falkner-Skan cross nanofluid reduces for larger magnitudes of melting parameter$M$. The inspiration of Prandtl number Prversus thermal profile of speciesθ is shown in Fig. 11. It is cleared that thermal field θdepressed by enhancing the values of Prandtl numberPr. Fig. 12 depicts the variation of temperature field of speciesθ for different magnitudes of temperature ratio parameterθ_w. It is clearly examines that temperature field of speciesθ exaggerates with an increase in temperature ratio parameterθ_w. Figs. 13 and 14 are plotted to scrutinize the behavior of melting parameter $M$and Lewis numberLe on solutal field of speciesϕ. It is analyzed that an enhancement in both parameters melting parameter $M$and Lewis numberLe depresses the solutal profile of nanomaterialsϕ. Fig. 15 examines the behavior of Brownian motion parameterNbon solutal field of nanoparticlesϕ. It is analyzed that solutal field of speciesϕ dwindle when Brownian motionNb is improved. Fig. 16 displays the impacts of thermophoresis parameterNt on volumetric concentration of nanoparticlesϕ. Here, it in noted that concentration field of speciesϕ enhanced by increasing the values of thermophoresis parameterNt. Fig. 17 is developing to illustrate the inspiration of Prandtl parameterPr versus solutal field of nanoparticlesϕ. Here solutal fieldϕ decreases by growing the estimation of Prandtl parameterPr.

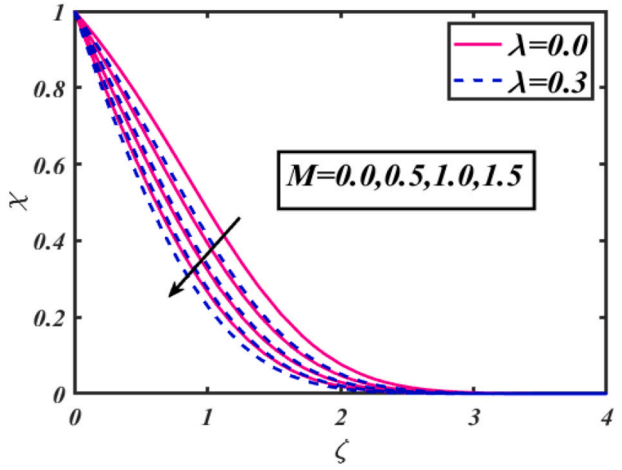

Fig. 18. Aspects of χvia$M$.

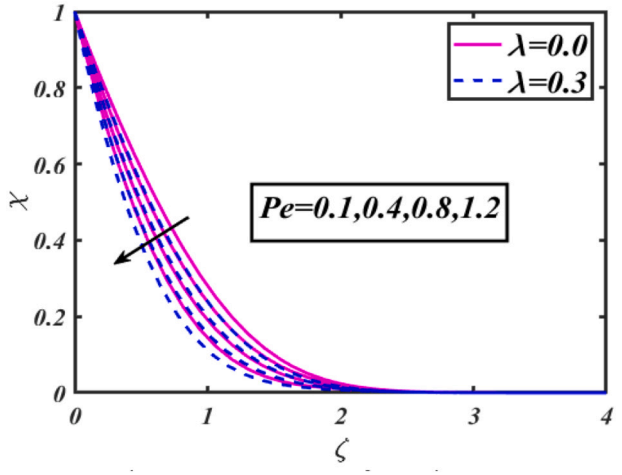

Fig. 19. Aspects of χviaPe.

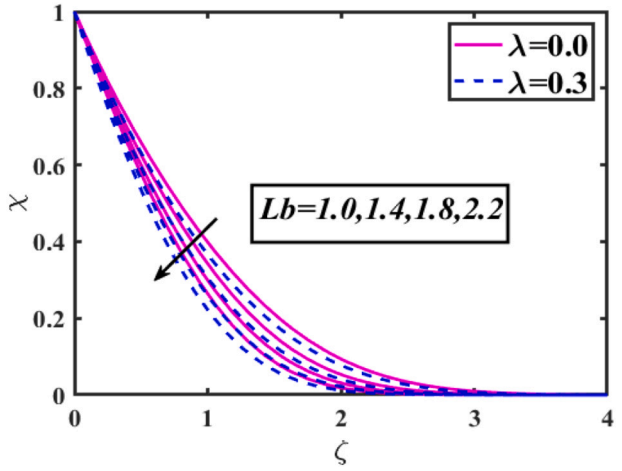

Fig. 20. Aspects of χviaLb.

Fig. 18 reports the impact of melting parameter$M$ against microorganism field $\chi$for both situations static$\lambda = 0.0$ and moving$\lambda = 0.3$ wedge. Clearly from the picture, it is found that microorganism's field $\chi$of Falkner-Skan nanofluid becomes decreased for growing the melting parameter$M$. Features of Peclet number Pevia microorganism fieldχ is reported through Fig. 19. It is seen from Fig. 20, as arising Peclet number Pedeclines the microorganism fieldχ for both conditions static wedge and moving wedge. Fig. 21 examines the effects of bioconvection Lewis numberLb against microorganism fieldχ of nanofluid across Wedge for both situations static and moving wedge. Here microorganism fieldχ decreased with larger bioconvection Lewis numberLb.

Table 1
Numerical estimation of local skin friction coefficient against different parameters values.

Parameters					$-f''(0)$
We	α	Nr	Nc	M	
0.1	0.1	0.1	0.1	2.0	1.1318
0.2					1.1314
0.4					1.1310
0.3	0.2	0.1	0.1	2.0	1.1189
	0.3				1.1045
	0.4				1.0901
0.3	0.1	0.5	0.1	2.0	1.1282
		1.0			1.1218
		1.5			1.1156
0.3	0.1	0.1	0.5	2.0	1.1469
			1.0		1.1639
			1.5		1.1156
0.3	0.1	0.1	0.1	2.5	1.2335
				3.0	1.3243
				3.5	1.4101

Table 2
Numerical estimation of local Nusselt number against different parameters values.

Parameters									$-\theta'(0)$
Pr	α	Nr	Nc	M	Rd	Nb	Nt	Bi	
2.5	0.1	0.1	0.1	2.0	0.4	0.5	0.3	2.0	1.0435
3.0									1.1135
3.5									1.1771
2.0	0.2	0.1	0.1	2.0	0.4	0.5	0.3	2.0	0.8687
	0.3								0.8681
	0.4								0.8674
2.0	0.1	0.5	0.1	2.0	0.4	0.5	0.3	2.0	0.8692
		1.0							0.8690
		1.5							0.8688
2.0	0.1	0.1	0.5	2.0	0.4	0.5	0.3	2.0	0.8700
			1.0						0.8708
			1.5						0.8718
2.0	0.1	0.1	0.1	2.5	0.4	0.5	0.3	2.0	0.8738
				3.0					0.8777
				3.5					0.8811
2.0	0.1	0.1	0.1	2.0	0.5	0.5	0.3	2.0	0.8539
					1.0				0.7909
					1.5				0.7434
2.0	0.1	0.1	0.1	2.0	0.4	0.1	0.3	2.0	0.8102
						0.2			0.8294
						0.3			0.8615
2.0	0.1	0.1	0.1	2.0	0.4	0.5	0.1	2.0	0.9721
							0.4		0.8476
							0.7		0.7993
2.0	0.1	0.1	0.1	2.0	0.4	0.5	0.3	2.5	0.9481
								3.0	1.0085
								3.5	1.0562

The numerical result of local skin friction coefficient, local Nusselt number, local Sherwood number and local micrdoorganisms density number against different magnitudes parameters are calculated numerical. Table 1 depicts that local skin friction reduces for larger αwhile it improve for M. Table 2 conveys the change in local Nusselt number which claim that it enhance for higher values of Pr and Nb. The local Sherwood number increase with Nc and M and shown in Table 3. Table 4 results the change in local microorganism density number which report that it increases with $Pe$and Lb.

Table 3
Numerical estimation of local Sherwood number against different parameters values.

Parameters								$-\phi'(0)$
Pr	α	Nr	Nc	M	Nb	Nt	Le	
2.5	0.1	0.1	0.1	2.0	0.5	0.3	1.0	2.6185
3.0								2.8547
3.5								3.0742
2.0	0.2	0.1	0.1	2.0	0.5	0.3	1.0	1.7065
	0.3							1.7047
	0.4							1.7028
2.0	0.1	0.5	0.1	2.0	0.5	0.3	1.0	1.7078
		1.0						1.7071
		1.5						1.7065
2.0	0.1	0.1	0.5	2.0	0.5	0.3	1.0	1.7102
			1.0					1.7125
			1.5					1.7148
2.0	0.1	0.1	0.1	2.5	0.5	0.3	1.0	1.7211
				3.0				1.7223
				3.5				1.7424
2.0	0.1	0.1	0.1	2.0	0.1	0.3	1.0	1.7509
					0.2			1.5014
					0.3			1.6975
2.0	0.1	0.1	0.1	2.0	0.5	0.1	1.0	3.7633
						0.4		1.5448
						0.7		1.4887
2.0	0.1	0.1	0.1	2.0	0.5	0.3	2.0	2.0384
							3.0	2.3070
							4.0	2.5390

Table 4
Numerical estimation of local microorganism density number against different parameters values.

Parameters							$-\chi'(0)$
We	α	Nr	Nc	M	Lb	Pe	
0.1	0.1	0.1	0.1	2.0	2.0	0.1	1.0331
0.2							1.0354
0.4							1.0394
0.3	0.2	0.1	0.1	2.0	2.0	0.1	1.0322
	0.3						1.0308
	0.4						1.0295
0.3	0.1	0.5	0.1	2.0	2.0	0.1	1.0332
		1.0					1.0328
		1.5					1.0325
0.3	0.1	0.1	0.5	2.0	2.0	0.1	1.0350
			1.0				1.0369
			1.5				1.0388
0.3	0.1	0.1	0.1	2.5	2.0	0.1	1.0429
				3.0			1.0519
				3.5			1.0594
0.3	0.1	0.1	0.1	2.0	3.0	0.1	1.1995
					4.0		1.3366
					5.0		1.4556
0.3	0.1	0.1	0.1	2.0	2.0	0.2	1.1813
						0.3	1.3309
						0.4	1.4820

5. Conclusions

A numerical interpretation of Falkner-Skan flow of cross nanofluid flow across a wedge under the static and moving conditions is examined in this work. The manifestation of gyrotactic motile microorganisms, activation energy, Brownian and thermophoresis diffusion and melting heat transfer are taken into acount. Main outcomes are listed via following points:

- The velocity profile enhanced for improving values of wedge angle parameter for both cases static and moving wedge.
- The infinite shear rate viscosity, bioconvection Rayleigh number and buoyancy ratio parameter declined the velocity of Falkner-Skan nanofluid.
- Velocity for melting parameter and mixed convection parameter is boosted up.
- For larger melting parameter and Prandtl number the thermal field is declined while raised with thermophoresis parameter.
- Solutel field of nanoparticles were depressed for Brownian motion parameter and Lewis number.
- The microorganism field was decreased with the augmentation of melting parameter, peclet number and bioconvection Lewis number.

Availability of data and materials

The data that support the findings of this study are available within the article; the data are made by the authors themselves and do not involve references of others.

Funding

Not applicable.

Author contributions

Not applicable.

Declaration of Competing Interest

The author declared that it has no conflict of interest.

Acknowledgments

The research was supported by the National Natural Science Foundation of China (Grant Nos. 11971142, 11871202, 61673169, 11701176, 11626101, 11601485).

References

[1] S. Choi, J. Eastman, Enhancing thermal conductivity of fluids with nanoparticles, in: Proceedings of the ASME International Mechanical Engineering Congress and Exposition, SanFrancisco, CA, USA,12–17, November 1995.
[2] J. Buongiorno, Convective transport in nanofluids, J. Heat Transf. 128 (2006) 240–250.
[3] Z. Li, F. Selimefendigil, M. Sheikholeslami, A. Shafee, M. Alghamdi, Hydrothermal analysis of nanoparticles transportation through a porous compound cavity utilizing two temperature model and radiation heat transfer under the effects of magnetic field, Microsyst. Technol. 26 (2) (2020) 333–344.
[4] I. Rashid, M. Sagheer, S. Hussain, Exact solution of stagnation point flow of MHD cu–H2O nanofluid induced by an exponential stretching sheet with thermal conductivity, Phys. Scr. 95 (2) (2020), 025207.
[5] T. Gul, M.Z. Ullah, A.K. Alzahrani, Z. Zaheer, I.S. Amiri, MHD thin film flow of kerosene oil based CNTs nanofluid under the influence of Marangoni convection, Phys. Scr. 95 (1) (2020), 015702.
[6] A.A. Siddiqui, A.J. Chamkha, Thermo-magnetohydrodynamic effects on cu+ engine oil/water nanofluid flow in a porous media-filled annular region bounded by two rotating cylinders, Proc. Inst. Mech. Eng. C J. Mech. Eng. Sci. (2020), 0954406220906435.
[7] X. Hu, D. Yin, J. Xie, X. Chen, C. Bai, Experimental study of viscosity characteristics of graphite/engine oil (5 W-40) nanofluids, Appl. Nanosci. (2020) 1–14.
[8] Ansari, M. S., Magagula, V. M., & Trivedi, M. Jeffrey nanofluid flow near a Riga plate: spectral quasilinearization approach. Heat Transf.—Asian Res.
[9] H.W. Xian, N.A.C. Sidik, R. Saidur, Impact of different surfactants and ultrasonication time on the stability and thermophysical properties of hybrid nanofluids, Intern. Commun. Heat Mass Transf. 110 (2020), 104389.
[10] S.O. Alharbi, Influence of wall slip and jump in wall temperature on transport of heat energy in hybrid nanofluid, J. Therm. Anal. Calorim. (2020) 1–8.
[11] M. Khan, T. Salahuddin, M.Y. Malik, A. Tanveer, A. Hussain, A.S. Alqahtani, 3-D axisymmetric Carreau nanofluid flow near the Homann stagnation region along with chemical reaction: application Fourier's and Fick's laws, Math. Comput. Simul. 170 (2020) 221–235.
[12] T.K. Nguyen, M. Usman, M. Sheikholeslami, R.U. Haq, A. Shafee, A.K. Jilani, I. Tlili, Numerical analysis of MHD flow and nanoparticle migration within a permeable space containing non-equilibrium model, Phys. A: Statist. Mech. App. 537 (2020), 122459.

[13] K.M. Rabbi, M. Sheikholeslami, A. Karim, A. Shafee, Z. Li, I. Tlili, Prediction of MHD flow and entropy generation by artificial neural network in square cavity with heater-sink for nanomaterial, Phys. A: Statist. Mech. Appl. 541 (2020), 123520.
[14] Ç. Demirkır, H. Ertürk, Rheological and thermal characterization of graphene-water nanofluids: hysteresis phenomenon, Int. J. Heat Mass Transf. 149 (2020), 119113.
[15] M. BarzegarGerdroodbary, Application of neural network on heat transfer enhancement of magnetohydrodynamic nanofluid, Heat Transf.—Asian Res. 49 (1) (2020) 197–212.
[16] R. Mustafin, A.D. Manasrah, G. Vitale, R. Askari, N.N. Nassar, Enhanced thermal conductivity and reduced viscosity of aegirine-based VR/VGO nanofluids for enhanced thermal oil recovery application, J. Pet. Sci. Eng. 185 (2020), 106569.
[17] Bestman, Natural convection boundary layer with suction and mass transfer in porous medium, Int. J. Eng. Res. 14 (1990) 389–396.
[18] Z. Shah, P. Kumam, W. Deebani, Radiative MHD Casson Nanofluid flow with activation energy and chemical reaction over past nonlinearly stretching surface through entropy generation, Sci. Rep. 10 (1) (2020) 1–14.
[19] R. Muhammad, M.I. Khan, M. Jameel, N.B. Khan, Fully developed Darcy-Forchheimer mixed convective flow over a curved surface with activation energy and entropy generation, Comput. Methods Prog. Biomed. 188 (2020), 105298.
[20] T. Muhammad, H. Waqas, S.A. Khan, R. Ellahi, S.M. Sait, Significance of nonlinear thermal radiation in 3D Eyring–Powell nanofluid flow with Arrhenius activation energy, J. Therm. Anal. Calorim. (2020) 1–16.
[21] W.A. Khan, M. Ali, M. Shahzad, F. Sultan, M. Irfan, Z. Asghar, A note on activation energy and magnetic dipole aspects for cross nanofluid subjected to cylindrical surface, Appl. Nanosci. 10 (8) (2020) 3235–3244.
[22] M.M. Bhatti, A. Shahid, T. Abbas, S.Z. Alamri, R. Ellahi, Study of activation energy on the movement of gyrotactic microorganism in a magnetized nanofluids past a porous plate, Processes 8 (3) (2020) 328.
[23] J.R. Platt, "Bioconvection patterns" in cultures of free-swimming organisms, Science 133 (3466) (1961) 1766–1767.
[24] S.U. Khan, A. Rauf, S.A. Hehzad, Z. Abbas, T. Javed, Study of bioconvection flow in Oldroyd-B nanofluid with motile organisms and effective Prandtl approach, Phys. A Statist. Mech. Appl. (2019) 1–31.
[25] M.A. Mansour, A.M. Rashad, B. Mallikarjuna, A.K. Hussain, M. Aichouni, L. Kolsi, MHD mixed bioconvection in a square porous cavity filled by gyrotactic microorganisms, Intern. J. Heat Technol. 37 (2) (2019) 433–445.
[26] S. Zaman, M. Gul, Magnetohydrodynamic bioconvetive flow of Williamson nanofluid containing gyrotactic microorganisms subjected to thermal radiation and Newtonian conditions, J. Theor. Biol. 479 (2019) 22–28.
[27] H. Waqas, S.U. Khan, S.A. Shehzad, M. Imran, Significance of the nonlinear radiative flow of micropolar nanoparticles over porous surface with a gyrotactic microorganisms, activation energy, and Nield's condition, Heat Transf. Asian Res. (2019) 1–27.
[28] M. Ramzan, M. Mohammad, F. Howari, Magnetized suspended carbon nanotubes based nanofluid flow with bio-convection and entropy generation past a vertical cone, Sci. Rep. 9 (2019) 12225.
[29] M.D. Shamshuddin, S.R. Mishra, O.A. Beg, A. Kadir, Adomian decomposition method simulation of von Kármán swrling bioconvection nanofluid flow, J. Cent. South Univ. 26 (10) (2019) 2797–2813.
[30] S. Nadeem, M.N. Khan, N. Muhammad, S. Ahmad, Mathematical analysis of bio-convective micropolar nanofluid, J. Comput. Design Eng. 6 (3) (2019) 233–242.
[31] F. Ayodeji, A. Tope, O. Pele, Magneto-hydrodynamics (MHD) bioconvection nanofluid slip flow over a stretching sheet with thermophoresis, viscous dissipation and Brownian motion, Mach. Learn. Res. 4 (4) (2020) 51.
[32] S.E. Ahmed, Z.A. Raizah, Unsteady mixed nanobioconvection flow in a horizontal channel with its upper plate expanding or contracting: a revised model, Therm. Sci. 23 (5 Part B) (2019) 3283–3292.
[33] Z. Abdelmalek, S.U. Khan, H. Waqas, A. Riaz, I.A. Khan, I. Tlili, A mathematical model for bioconvection flow of Williamson nanofluid over a stretching cylinder featuring variable thermal conductivity, activation energy and second-order slip, J. Therm. Anal. Calorim. (2020) 1–13.
[34] S.U. Khan, H. Waqas, M.M. Bhatti, M. Imran, Bioconvection in the rheology of magnetized couple stress nanofluid featuring activation energy and Wu's slip, J. Non-Equilib. Thermodyn. 45 (1) (2020) 81–95.
[35] H. Waqas, S.U. Khan, I. Tlili, M. Awais, M.S. Shadloo, Significance of bioconvective and thermally dissipation flow of viscoelastic nanoparticles with activation energy features: novel biofuels significance, Symmetry 12 (2) (2020) 214.
[36] Z. Abdelmalek, S.U. Khan, H. Waqas, A. Riaz, I.A. Khan, I. Tlili, A mathematical model for bioconvection flow of Williamson nanofluid over a stretching cylinder featuring variable thermal conductivity, activation energy and second-order slip, J. Therm. Anal. Calorim. (2020) 1–13.
[37] H. Waqas, S.U. Khan, S.A. Shehzad, M. Imran, Radiative flow of Maxwell nanofluid containing gyrotactic microorganism and energy activation with convective Nield conditions, Heat Transf.—Asian Res. 48 (5) (2019) 1663–1687.
[38] Muhammad Sadiq Hashmi, Kamel AL-Khaled, Nargis Khan, Sami Ullah Khan, Iskander Tlili, Buoyancy driven mixed convection flow of magnetized Maxell fluid with homogeneous-heterogeneous reactions with convective boundary conditions, Results Phys. 19 (December 2020) 103379.
[39] Zoubair Boulahia AbderrahimWakif, Rachid SehaquiA semi-analytical analysis of electro-thermo-hydrodynamic stability in dielectric nanofluids using Buongiorno's mathematical model together with more realistic boundary conditions, Results Phys. 9 (June 2018) 1438–1454.
[40] A. Mahdy, A. Hossam, Nabwey,Microorganisms time-mixed convection nanofluid flow by the stagnation domain of an impulsively rotating sphere due to Newtonian heating, Results Phys. 19 (December 2020), 103347.